International Journal of
Scientific Research in Science and Technology (IJSRST)
Print ISSN : 2395-6011, Online ISSN : 2395-602X
International Conference on Advanced Materials
Held on 14, 15 December 2017, Organized by Department of Physics,
St. Joseph's College, Trichy, Tamilnadu, India

Synthesis and Characterization of Cerium doped $CaMnO_3$ Nanoparticles

S. Berbeth Mary, A. Leo Rajesh*

Department of Physics, St. Joseph's College (Autonomous), Tiruchirappalli-620 002, Tamil Nadu, India

*corresponding author: E-mail address: aleorajesh@gmail.com;

Tel.:+91-944412207

Abstract

Nanostructured cerium doped calcium manganite $Ca_{1-x}Ce_xMnO_3$ (x=0.0, 0.1, 0.2, 0.3, 0.4, 0.5) samples were synthesized successfully using the citric acid complexing coupled with hydrothermal method followed by annealing at 900°C. Powder X-ray diffraction (XRD) analysis showed that the single phases of orthorhombic pervoskite structure of $CaMnO_3$ and the cell volume increased from undoped to cerium doped $CaMnO_3$ structure due to the ionic radius of added R^{3+} cations. The crystallinity decreased with increased concentration of Ce^{3+} doping and the average crystallite size was about 10-20 nm. Sphere like nanoparticles observed by the scanning electron microscopy. FTIR analysis showed a strong peak around 600 cm^{-1} revealed the formation of pervoskite oxides and the obtained band gap was 3.56 eV.

Keywords: calcium manganite, hydrothermal, single phase, pervoskite oxide

1. Introduction

The development of environmental friendly and cost effective power sources overcomes the problems of energy crises and global warming. Thermoelectric power generation is a promising method by converting waste heat directly into electricity without any greenhouse gas emission. The conversion efficiency is measured by the dimensionless figure of merit

$$ZT = \left(\frac{S^2\sigma}{k}\right)T$$

where S, σ, K, T are seebeck coefficient, electrical conductivity, thermal conductivity and absolute temperature respectively. Good thermoelectric materials should have large seebeck coefficient, high electrical conductivity and low thermal conductivity where large electrical conductivity minimize joule heating while low thermal conductivity maintains temperature gradient between the hot and cold sides in thermoelectric device. The intermetallic materials such as Bi_2Te_3 and $CoSb_3$ have high ZT at low temperatures. However, they are toxic, rare and degrade at high temperatures under air [1]. Besides, thermoelectric materials are required to be stable at higher temperatures. Oxides are one of the best candidate materials for this requirement but most oxides with high stability at high temperature in air are unsuitable for thermoelectric applications due to high electrical resistivity. These limitations were overcomed by the discovery of Na_xCoO_2 with a high seebeck coefficient (100mV/K at 300 K) and a low electrical resistivity (0.2 m Ω at 300K) by Terasaki et al in 1997 [2].

The interesting physical properties such as electrical, electrochemical, magnetic, superconducting and thermoelectrical make them great candidates in various energy storage applications like supercapacitor, solid oxide fuel cells and thermoelectric devices [3-5]. Several pervoskite type oxides are well known as highly conductive ceramics whereas $CaMnO_3$ based oxides are the major n-type thermoelectric oxide which produces granular fine particles with high chemical and thermal stability. The undoped

International Journal of
Scientific Research in Science and Technology (IJSRST)
Print ISSN : 2395-6011, Online ISSN : 2395-602X
International Conference on Advanced Materials
Held on 14, 15 December 2017, Organized by Department of Physics,
St. Joseph's College, Trichy, Tamilnadu, India

$CaMnO_3$ has poor TE property due to the high electrical resistivity whereas calcium substitution with various rear earth elements can enhance the carrier mobility which progress the electrical conductivity [6]. The thermoelectric performance of pervoskite type oxides can be enhanced by doping, band engineering and nanostructuring [7]. Reduction of thermal conductivity can be accomplished by nanotailoring with controlled grain size. $Ca_{1-x}Re_xMnO_3$ can be successfully synthesized by various bottom up methods such as chemical combustion, sol-gel, coprecipitation, hydrothermal method and so on [8-11]. Here citric acid complexing coupled with hydrothermal method has been employed to obtain high purity, homogenous, environmental friendly and fine particles with controlled grain size [12 -14].

$CaMnO_3$ based thermoelectric materials has high seebeck coefficient but the dimensionless figure of merit is low because of low electrical conductivity. N- type doping at A-site (Ca), B-site (Mn) and dual doping at both sites has been done to improve the TE property, while A- site rare earth elements doping shows the enhancement in ZT values [15-18]. In rare earth doped manganite, dopant occupies either A-site or B-site depending on its radius. Doping cerium in $CaMnO_3$, Ce occupies the A-site and raises the Thermoelectric (TE) performance by strongly reducing the resistivity [19]. In this paper, the effects of Ce substitution on nanostructured n-type thermoelectric oxide $Ca_{1-x}Ce_xMnO_3$ (CCMO) samples are systematically studied.

2. Materials and Methods

$Ca_{1-x}Ce_xMnO_3$ (x=0.0, 0.1, 0.2, 0.3, 0.4, 0.5) powders were prepared using the strategy of citric acid complexing coupled with hydrothermal method. Stoichiometric amounts of nitrates such as cerium, calcium, manganese and equal amount of citric acid (metal/citric acid molar ratio = 1/1) were dissolved in deionized water to obtain homogeneity in the metal ions. A certain amount of ammonia solution was added drop wise to the above mixed solution. Part of ammonia added to neutralize the unreacted citric acid. When the pH value of the solution reached around 9.2 a sol was obtained. This sol was transferred to a 150 ml stainless steel autoclave was placed it in hot air oven at 200 °C for 20 hr. once the assigned time was over the oven was switched off and allowed to cool down to room temperature. The obtained products were in turn filtered, washed with deionized water and ethanol, filtered again, and dried around 120 °C overnight. The dried powders were well ground and annealed in air at 900 °C for 4 hr.

Crystal structure and phase identification were determined by Powder X-ray diffraction (XRD) and data were collected using a XRD diffractometer (D8 Advanced) with CuKα radiation (λ =0.15406 nm). The surface morphology was observed with scanning electron microscopy (SEM). Fourier transform infrared (FTIR) spectra of the powder samples were recorded from 4000 to 400 cm^{-1} using a Fourier transform infrared spectrometer (Perkin Elmer) equipped with a KBr beam splitter. The optical properties of the nanoparticles were characterized by UV-Vis spectroscopy Lambda 35 UV-Vis spectrometer.

3. Results and Discussion

The yellowish colour of the manganese nitrate solution is turned into bluish when pH value of the solution reached to 9.2. After centrifugation and drying, the powder is darkish due to the presence of different manganese valance states [20]. Figure 1

International Journal of
Scientific Research in Science and Technology (IJSRST)
Print ISSN : 2395-6011, Online ISSN : 2395-602X
International Conference on Advanced Materials
Held on 14, 15 December 2017, Organized by Department of Physics,
St. Joseph's College, Trichy, Tamilnadu, India

represents the XRD patterns of annealed undoped and doped $CaMnO_3$ powders. They clearly demonstrate the single phase of orthorhombic pervoskite structure of $CaMnO_3$ which is matching with JCPDS Card no 76-1133 with space group Pnma, indicating that annealing under oxygen atmosphere leads to the formation of $CaMnO_3$ structure [21]. The strong doublet of the main pervoskite peak in the 2θ region, 33° of the CCMO nanostructure exhibited a tendency to unify with increasing the doping concentration [22, 23]. Fig 1(d) shows that there is shift in peaks due to the release of large volume of gases while annealing.

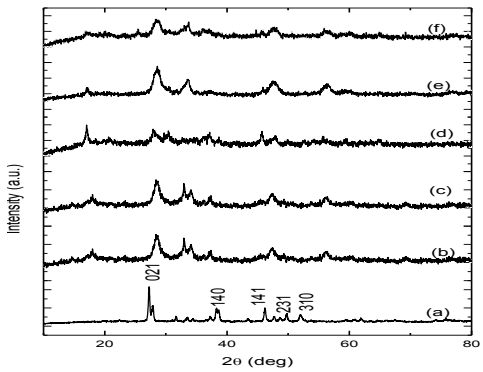

Figure 1. XRD Pattern of $Ca_{1-x}Ce_xMnO_3$ (x = 0.0, 0.1, 0.2, 0.3, 0.4, 0.5) samples

The average grain size of the synthesized samples are calculated from the major diffraction peaks using the Scherrer formula $D = K\lambda/\beta\cos\theta$, where K is constant (K = 0.94), λ is the wavelength (1.5406 Å). θ is the Bragg angle; β is full width half maximum that is, broadening due to the crystallite dimensions [24]. The average grain size of the prepared samples is in the range of 10-20 nm. Partial substitution of Ce^{3+} (Ln^{3+}) for Ca^{2+} decreases the average grain size with increasing the cerium concentration [25-27].

Figure 2 shows SEM images of undoped and cerium doped $CaMnO_3$ samples. It can be seen that all the samples shows a porous nature. This porous morphology is attributed to the release of a large volume of gases during the synthetic process due to the addition of citric acid as chelating agent and post heating treatment. The majority of the particles are nearly round shaped and the others are elongated. The average size of spherical particles deduced from SEM lies in the range of few nanometers. Microstructures of cerium doped samples are downgraded, which is associated with the most decrease of electrical conductivity. The decrease of electrical conductivity leads to a decrease of κ_e, which is due to the partial substitution of Ce^{3+} for Ca^{2+}, the decrease of κ_{total} can be mainly attributed to the reduction of lattice contribution arising from incorporation of heavier Ce^{3+} ions in the structure as compared to Ca^{2+} ions [28] ($\kappa_{total} = \kappa_{ph} + \kappa_e$, where κ_e and κ_e are the thermal conductivity due to lattice and electronic contribution) which leads to the enhancement in thermo power S.

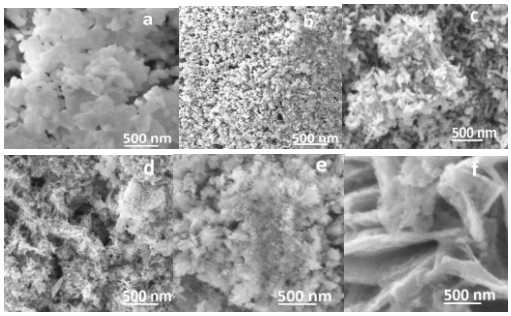

Figure 2. SEM Micrograph of $Ca_{1-x}Ce_xMnO_3$ (x = 0.0, 0.1, 0.2, 0.3, 0.4, 0.5) samples

The FTIR study is carried out to correlate the relative change in the high frequency stretching mode and mid frequency bending mode with the bond lengths and consequently to the unit cell volume [29, 30]. Figure 3 shows the FTIR spectra of CCMO nanoparticles. The typical peak of CCMO nanoparticle is observed around 500-600 cm^{-1}. The symmetric stretching occurs about 800 cm^{-1} indicates the vibration of NO_3^{-1} ions. The strong

International Journal of
Scientific Research in Science and Technology (IJSRST)
Print ISSN : 2395-6011, Online ISSN : 2395-602X
International Conference on Advanced Materials
Held on 14, 15 December 2017, Organized by Department of Physics,
St. Joseph's College, Trichy, Tamilnadu, India

asymmetric stretching mode of vibration of C=O is observed around 1300-1500 cm^{-1}. The band at 3500 cm^{-1} corresponds to O-H mode of vibration [31,32].

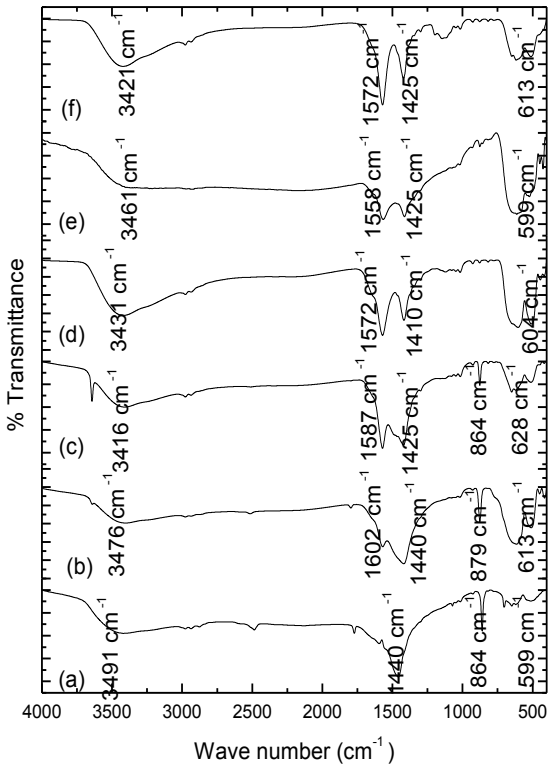

Figure 3. FTIR Spectra of $Ca_{1-x}Ce_xMnO_3$ (x = 0.0, 0.1, 0.2, 0.3, 0.4, 0.5) samples

Figure 4(a) shows UV-Visible spectra of $Ca_{1-x}Ce_xMnO_3$ nanoparticles. The absorption peaks are around 300 cm^{-1}. When the concentration of cerium increases peak value also increases. The band gap E_g can be calculated from the equation

$$(\alpha h\upsilon)^n = B(h\nu - E_g)$$

where α is absorption coefficient, $h\nu$ is the photon energy, B is constant, and n can be either 1/2 or 2 for indirect and direct transitions respectively [33]. The $(\alpha h\nu)^2$ versus $h\nu$ curve is shown in figure 4(b) and it is found to be 3.56 eV which is good agreement with the optimum value. These results show that this material it is suitable for thermoelectric application.

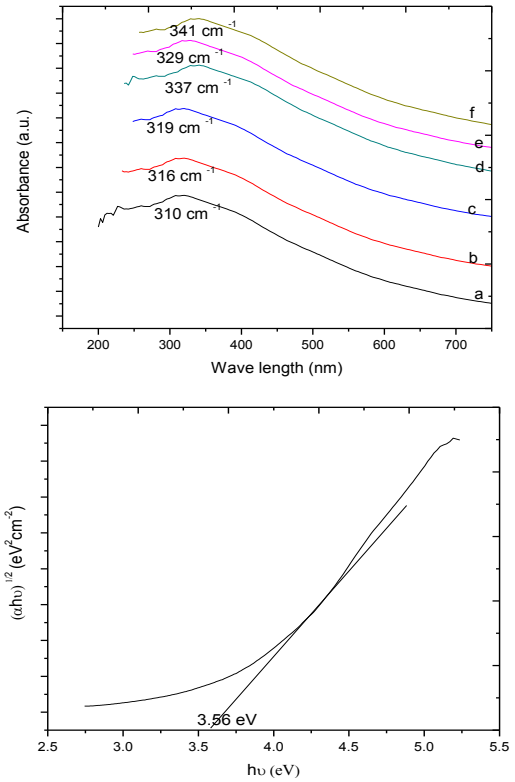

Figure 4(a). UV- Visible Spectra of $Ca_{1-x}Ce_xMnO_3$ (b) Band gap determination

4. Conclusion

This work exhibited that Cerium is a suitable alternative material for Ca in $Ca_{1-x}Ce_xMnO_3$,, here the concentration was ($x \leq 0.5$) in which there is no chance in the crystal structure and the improved thermoelectric properties were obtained using citric acid complexing coupled with hydrothermal method. Crystalline and single phase structure of the nanoparticle was observed for all the samples. The observed porous nanoparticles lead to the connectivity in microstructure due to chelating reagent. The peaks at 600 cm^{-1} concluded the presence of Cerium doped $CaMnO_3$ nanoparticle and the band gap energy was calculated t o be 3.56 eV. The crystalline nature, porosity and low band

gap nature of these samples confirms that it is suitable for thermoelectric application. Sphere shaped surface morphology was observed for majority of the samples. The chelating agent played major role obtains the reduced particle size and good porous nature of the material.

References

[1] G. Chen, M. S. Dresselhaus, D. Dresselhaus, J.P. Fleurial, T. Caillat, Int. Mater. Rev., 48, 45 (2003).

[2] J. Pei, G. Chen, N. Zhou, D.Q. Lu, F.Q Xiao, Physica B., 406, 571 (2011)

[3] M.A. Pena, J.L.G. Flerro, Chem. Rev., 101, 7 (2001)

[4] E. Konysheva, J.T.S. Irvine, J. Mater. Chem., 18, 5147 (2008).

[5] F. Azough, C. Leach, R. Freer, J. Eur. Ceram. Soc., 26, 10 (2006).

[6] J. Dho, W.S. Kim, E.O. Chi, N.H. Hur, S.H. Park, H.-C. Ri, Solid State Commun., 125, 143 (2003)

[7] Michitaka Ohtaki, Hisako Koga, Tsutomu Tokunaga, Koichi Eguchi, Hiromichi Arai, J. Solid State Chem., 120, 105 (1995)

[8] R.V. Mangalaraja, J. Mouzon, P. Hedström, I. Kero, K.V.S. Ramam, C.P. Camurri, M. Odén, J. Mater. Process. Technol., 208 415 (2008)

[9] N.P. Bansal, J. Mater. Sci. 27, 2922 (1992)

[10] C.S. Sanmathi, Y. Takahashi, D. Sawaki, Y. Klein, R. Retoux, I. Terasaki, J.G. Noudem, Mater. Res. Bull., 45, 558 (2010)

[11] Jianrong Niu, Jiguang Deng, Wei Liu, Lei Zhang, Guozhi Wang, Hongxing Dai, Hong He, Xuehong Zi, Catal. Today., 126, 420 (2007)

[12] Yoshimura M, Yoo S. E, Hayashi M, Ishizawa N, J. Appl. Phys., 28, 2007 (1989)

[13] Sridhar Komarneni , Young Dong Noh , Joo Young Kim , Seok Han Kim , Hiroaki Katsuki, Naturforsch., 65b, 1033 (2010)

[14] A. Pathak , P. Pramanik, Pinsa., 67, 47 (2001)

[15] T. Okuda, Y. Fujii, J. Appl. Phys., 108, 103702 (2010)

[16] D. Sousa, M.R. Nunes, C. Silveira, I. Matos, A.B. Lopes, M.E. Jorge, Mater. Chem. Phys., 109, 311 (2008)

[17] G. Xu, R. Funahashi, Q. Pu, B. Liu, R. Tao, G. Wang, Z. Ding, Solid State Ionics., 171, 147 (2004).

[18] Y.H. Zhu, C.L. Wang, W.B. Su, J.C. Li, J. Liu, Y.L. Du, L.M. Mei, Ceram. Int., 40, 15531 (2014)

[19] Mohamed Mouyane, Brahim Itaalit, Jérôme Bernard, David Houivet, Jacques G. Noudem, Powder Technology., 264 ,71 (2014)

[20] Ma R, Takada K, Fukuda K, Iyi N, Bando Y, Sasaki T, Angew, Chem. Int. Ed., 47, 86 (2008)

[21] Mohamed Mouyane, Brahim Itaalit, Jerome Bernad, David Houuivet, Jacques G Noudem, Powder Tech., 264, 71 (2014)

[22] Millini R, Gagliardi MF, Piro G, J. Mater. Sci., 29, 4065 (1994)

[23] Gaudon M, Laberty-Robert C, Ansart F, Stevens P, Rousset A, Solid State Sci., 4, 125 (2002)

[24] S. Enzo, G. Fagherazzi, A. Benedetti, S. Polizzi, J. Appl. Cryst., 21, 536 (1988)

[25] N.V. Nong, Chia Jyi Liu, M. Othaki, J. Alloys. Compds., 509, 977 (2011)

[26] W. Koshibae, K. Tsutsui, S. Maekawa, Phys. Rev. B., 62, 6869 (2000)

[27] R. Asahi, J. Sugiyama, T. Tani, Phys. Rev. B., 66, 155103 (2002)

[28] R. K. Gupta, C.M. Whang, Solid State Ionics., 178, 1617 (2007)

[29] M. Daturi, G. Busca, R. J. Willey, Chem. Mater., 7, 2115 (1995)

[30] Rizwan Wahab, Young-Soon Kim, Hyung-Shik Shin, Mater.Trans., 50, 2092 (2009)

[31] G. De Marzi, Z. V. Popovic, A. Cantarero, Z. Dohcevic-Mitrovic N.Paunovic, J. Bok, F. Sapina, Phys. Rev. B., 68, 064302 (2003)

[32] K. Rekha, M. Nirmala, Manjula G.Nair, A. Anukaliani, Physica B, Cond Matr., 405, 3180 (2010)

[33] K. Omri, J. El Ghoul, O. M. Lemine, M. Bououdina, B. Zhang, L. El Mir, Superlattices and Microstructures., 60, 139 (2013)